Journal Pre-proofs

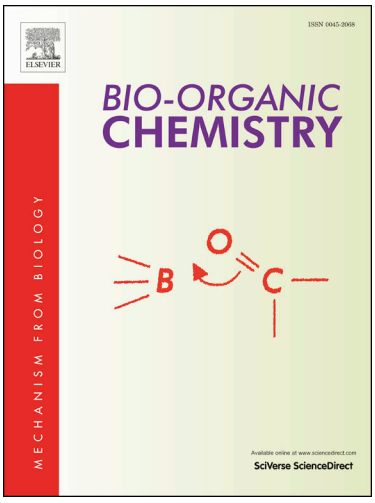

Design, synthesis and biological evaluation of pyridine derivatives as selective SHP2 inhibitors

Wen-Shan Liu, Bing Yang, Rui-Rui Wang, Wei-Ya Li, Yang-Chun Ma, Liang Zhou, Shan Du, Ying Ma, Run-Ling Wang

PII: S0045-2068(19)32039-5
DOI: https://doi.org/10.1016/j.bioorg.2020.103875
Reference: YBIOO 103875

To appear in: *Bioorganic Chemistry*

Received Date: 28 November 2019
Revised Date: 31 March 2020
Accepted Date: 21 April 2020

Please cite this article as: W-S. Liu, B. Yang, R-R. Wang, W-Y. Li, Y-C. Ma, L. Zhou, S. Du, Y. Ma, R-L. Wang, Design, synthesis and biological evaluation of pyridine derivatives as selective SHP2 inhibitors, *Bioorganic Chemistry* (2020), doi: https://doi.org/10.1016/j.bioorg.2020.103875

Design, synthesis and biological evaluation of pyridine derivatives as selective SHP2 inhibitors

Wen-Shan Liu[a, b, 1], Bing Yang[c,1], Rui-Rui Wang[a], Wei-Ya Li[a], Yang-Chun Ma[a], Liang Zhou[a], Shan Du[a], Ying Ma[a, *], Run-Ling Wang[a, *]

[a]Tianjin Key Laboratory on Technologies Enabling Development of Clinical Therapeutics and Diagnostics (Theranostics), School of Pharmacy, Tianjin Medical University, Tianjin 300070, China.

[b]Department of pharmacy, Affiliated Hospital of Weifang Medical University, Weifang, Shandong 261000, China.

[c]Department of Cell Biology, School of Basic Medical Science, Tianjin Medical University, Tianjin 300070, China.

[1]These authors contributed equally to this work.

[*]Correspondence to:

Ying Ma Email: maying@tmu.edu.cn

Run-Ling Wang Email: wangrunling@tmu.edu.cn

Funding information

Contract grant sponsor: National Natural Science Foundation of China; Contract grant number: 81773569.
Contract grant sponsor: Natural Science Foundation of Tianjin; Contract grant number: 16JCZDJC32500, 18JCQNJC13700.
Contract grant sponsor: Cooperation and Exchange Project of the National Natural Science Foundation of China; Contract grant number: 81611130090.
Contract grant sponsor: Science & Technology Development Fund of Tianjin Education Commission for Higher Education; Contract grant number: 2017KJ229.

Abstract

SHP2 is a non-receptor protein tyrosine phosphatase encoded by the PTPN11 gene, which affects the transduction of multiple signaling pathways, including RAS-ERK, PI3K-AKT and JAK-STAT. SHP2 also plays an important role in the programmed cell death pathway (PD-1 / PD-L1). Studies have shown that SHP2 is associated with a variety of cancers, including breast, liver and gastric cancers. Therefore, the development of SHP2 inhibitors has attracted extensive attention. In this study, based on the known inhibitor 1 (SHP099), novel SHP2 inhibitors were designed by means of scaffold hopping, and 35 pyridine derivatives as SHP2 inhibitors were found. The *in vitro* enzyme activity assay was performed on these compounds, and multiple selective SHP2 inhibitors with activity potency similar to that of SHP099 were obtained. Among them, compound (2-(4-(aminomethyl)piperidin-1-yl)-5-(2,3-dichlorophenyl)pyridin-3-yl)methanol (11a) was the most potent and highly selective SHP2 inhibitor with an *in vitro* enzyme activity IC_{50} value of 1.36 μM. Fluorescence titration assay verified that 11a bound directly to SHP2 protein. Subsequently, cell assay of representative compounds showed that these compounds could effectively inhibit the proliferation of Ba/F_3 cells. In addition, the pharmacokinetic characteristics of the designed compounds were analyzed by the *in silico* ADMET prediction. Molecular docking study provided more detailed information on the binding mode of compounds and SHP2 protein. In brief, this study reported for the first time that pyridine derivatives as novel SHP2 inhibitors had good inhibitory activity and selectivity, providing new clues for the development of small molecule SHP2 inhibitors.

Keywords: SHP2 inhibitor, scaffold hopping, activity, ADMET, molecular docking

1. Introduction

SHP2 is a non-receptor protein tyrosine phosphatase encoded by the *PTPN11* gene, which composes of two SH2 domains (N-SH2 and C-SH2), a catalytic PTP domain and a C-terminal tail that has at least two phosphorylation sites[1] [2]. X-ray crystallography studies have demonstrated that in the basal state, SHP2 adopts an auto-inhibited conformation, which the SH2 domain associates with the PTP domain and prevents substrates from accessing the active site[3]. Activation of SHP2 occurs through binding of bis-phosphotyrosyl peptides (e.g., IRS-1) to the SH2 domain, disrupting the interaction between the SH2 and PTP domains. The resulting conformational opening exposes the active site and increases phosphatase activity, which promotes cancer dependence[4].

Gain-of-function mutations in *PTPN11* that lead to hyperactivation of SHP2 have been identified in Noonan syndrome (50%)[5], juvenile myelomonocytic leukemia (JMML, 35%), myelodysplastic syndrome (10%), B-cell accute lymphoblastic leukemia (7%), acute myeloid leukemia (AML, 4%) [6]. In cell, SHP2 is located in the cytoplasm and transduces cell signaling from a variety of receptor–tyrosine kinases, and is therefore involved in numerous oncogenic cell signaling cascades, including RAS-ERK, PI3K-AKT and JAK-STAT [8, 9]. In addition, SHP2 is also involved in the programmed cell death pathway (PD-1/PD-L1) and contribute to immune evasion[10]. After PD-L1 is stimulated, SHP2 binds to PD-1 and inhibits T cell activation, making it a new target for cancer immunotherapy[11]. In view of the importance of SHP2 for human diseases, the development of small molecule SHP2 inhibitors has attracted widespread attention.

Due to the high homology between the SHP2 catalytic site and other tyrosine phosphatases,

targeting SHP2 small molecule inhibitors pose great challenges in achieving the selectivity between phosphatases. Moreover, the highly conserved and charged environment of SHP2 catalytic site greatly complicates drug development, resulting in the slow progress in the clinical study of SHP2 inhibitors[12, 13] [14]. The previously reported SHP2 inhibitors did not achieve the desired potency and selectivity, such as the first three compounds in Figure 1[15-17]. Until recently, a potent, selective, orally bioavailable inhibitor 1 (SHP099, IC_{50} = 70 nM) had been shown to inhibit cancer cell growth *in vitro* and in mouse tumor xenograft models and had entered clinical study, demonstrating that inhibition of SHP2 was an effective treatment for cancer. Interestingly, X-ray analysis of SHP099 and SHP2 protein revealed a new allosteric binding mode that inhibited SHP2 phosphorylation by stabilizing the self-inhibited conformation of SHP2[18, 19]. Based on this, the development of SHP2 allosteric inhibitors had been triggered, and many small-molecule compounds with high inhibitory activity and high selectivity have been developed, such as RMC-4550 (IC_{50} = 0.583 nM), which had been shown to inhibit RAS/MAPK signaling and slow down the growth of various cancer[20]. Currently, the inhibitor RMC-4550 had entered clinical trials. Other SHP2 allosteric inhibitors, such as SHP394 and SHP389, had good inhibitory potency and selectivity on SHP2 protein[21, 22]. Therefore, preventing the phosphorylation of SHP2 protein by stabilizing the autoinhibited conformation of SHP2 protein has become a new direction for the development of SHP2 inhibitors.

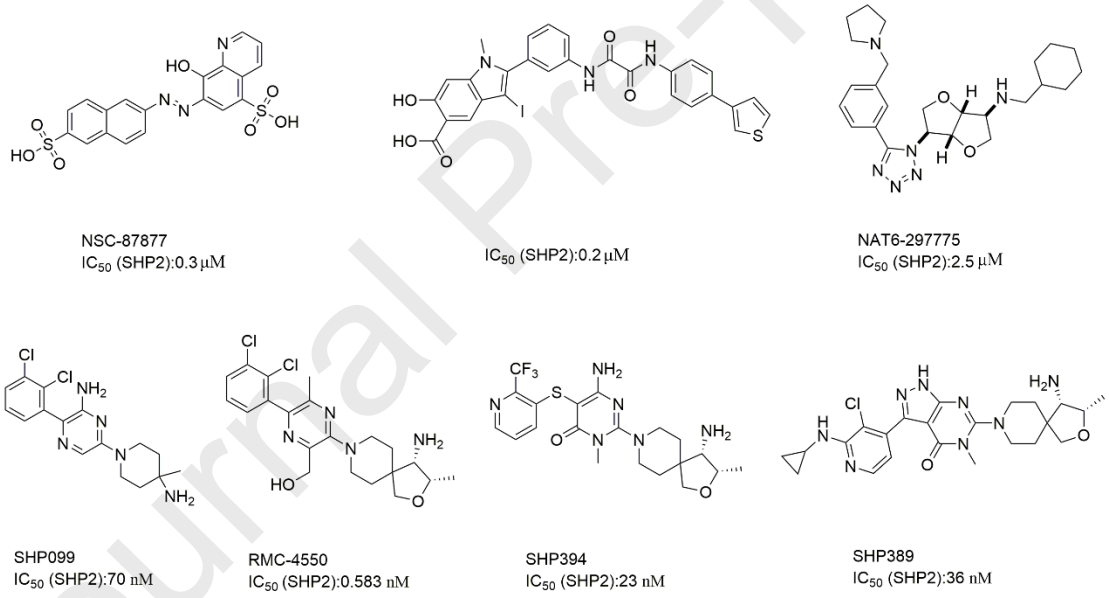

Figure 1. Representative SHP2 inhibitors that have been previously reported. Among them, the first three compounds are inhibitors against the catalytically active region of SHP2PTP, and the latter four compounds are inhibitors against the allosteric region of SHP2 protein.

Scaffold hopping is a very effective strategy that has been widely used to design potential bioactive molecules[23-25]. In this study, based on the known inhibitor SHP099, the SHP2 inhibitors with 3-substituted pyridine as the core structure was designed by scaffold hopping, as shown in Figure 2. In scaffold A, in addition to retaining the amino substituent, hydroxymethyl substituent was also introduced into the pyridine ring to increase structural diversity. Subsequently, 35 compounds were designed by fragment replacement of scaffolds B and C. Through the *in vitro* enzyme activity and cell proliferation assays on 35 designed compounds, it was identified that multiple compounds exhibited good inhibitory activity and selectivity for SHP2 protein. Fluorescence quenching assay

was performed on the compound 11a with the highest activity, demonstrating that the compound 11a would bind directly to SHP2 protein. Then, cell proliferation assay was performed on the representative compounds. Furthermore, these 35 compounds were confirmed to be drug-like by ADMET prediction. Molecular docking study provided more detailed information on the binding modes of compounds and SHP2 protein. In this paper, the pyridine derivatives as SHP2 inhibitors were studied for the first time, providing a new idea for the further development of small molecule SHP2 inhibitors.

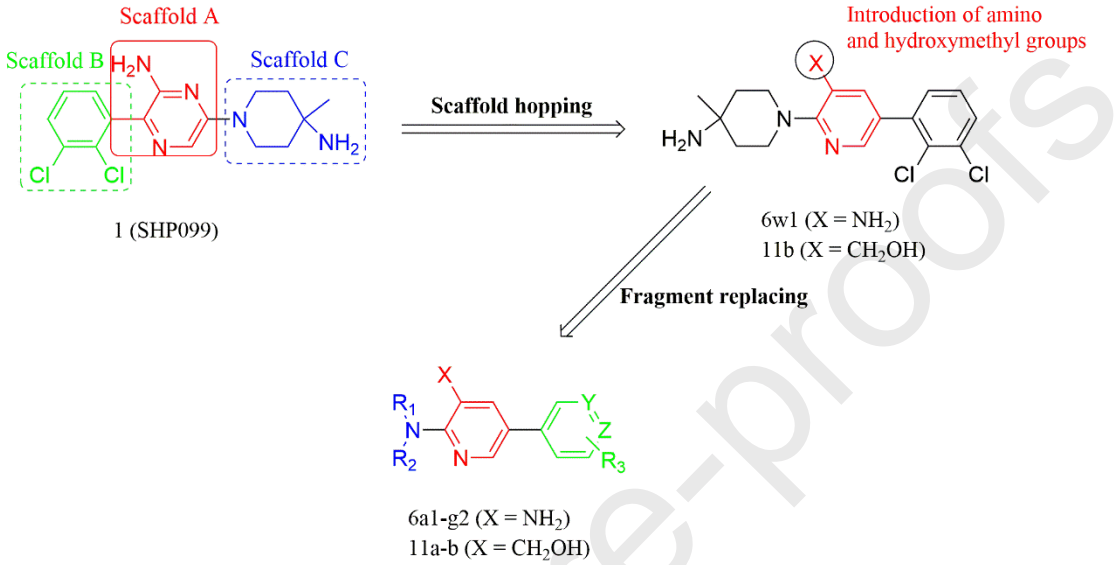

Figure 2. Design strategy of target compounds based on scaffold hopping.

2. Results and discussion

2.1. chemistry

These 35 target compounds were prepared by the synthetic route in schemes 1 and 2. Scheme 1 showed the synthetic route of compounds 6a1-g2, which used 5-bromo-2-chloro-3-nitropyridine as the starting material. First, in the presence of N, N-diisopropylethylamine (DIEA), the 2-position chlorine on the 5-bromo-2-chloro-3-nitropyridine was substituted by the nucleophilic substitution reaction to gain the intermediates 3a-j. The Suzuki-Miyaura coupling was carried out to obtain the intermediates 4ai-g2. Subsequently, the nitro group was reduced to amino group by zinc powder to obtain the intermediates 5a1-g2. Finally, in the presence of trifluoroacetic acid (TFA), Boc protecting groups were removed, and the target compounds 6a1-g2 were obtained.

Scheme 2 showed the synthetic route for compound 11a-b using methyl 5-bromo-2-chloronicotinate as starting material. First, the compound methyl 5-bromo-2-chloronicotinate (7) was subjected to the Suzuki-Miyaura coupling reaction with (2,3-dichlorophenyl)boronic acid to obtain Intermediate 8. Then, through nucleophilic substitution reaction, the intermediates 9a-b were obtained by replacing the 2-position chlorine on intermediate 8. Subsequently, the Boc protecting group on intermediates 9a-b were removed in the presence of trifluoroacetic acid to gain intermediates 10a-b. Finally, the ester group on the intermediates 10a-b were reduced to the hydroxyl group by the reducing agent lithium aluminum hydride to gain the target compounds 11a-b.

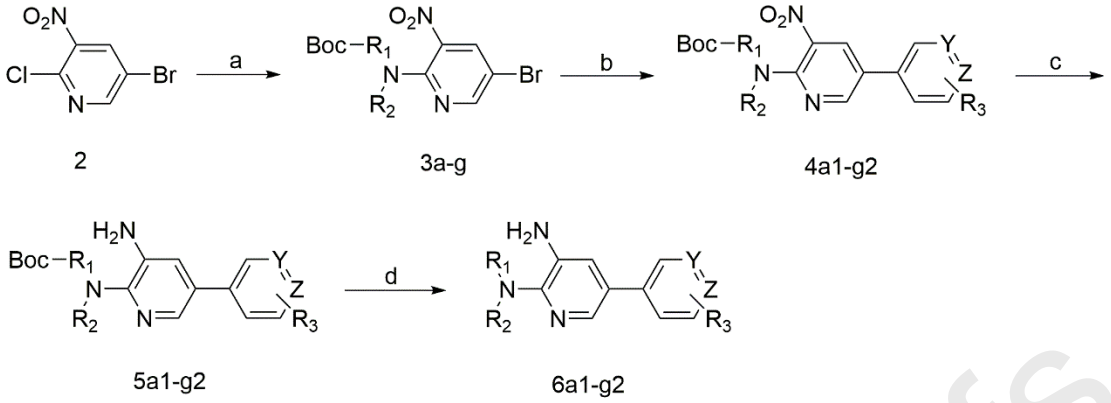

Scheme 1. Synthesis of the target compounds 6a1-g2. Reagents and condition: (a) NHR_1R_2Boc, DIEA, 1,4-Dioxane, 90°C, 87−91%; (b) $ArR_3B(OH)_2$, $Pd(PPh_3)_4$, K_2CO_3, 1,4-Dioxane/H_2O, 100°C, 82−89%; (c) zinc powder, NH_4Cl, EtOH, 80 °C, 85−93%; (d) TFA, DCM, rt, 87−92%.

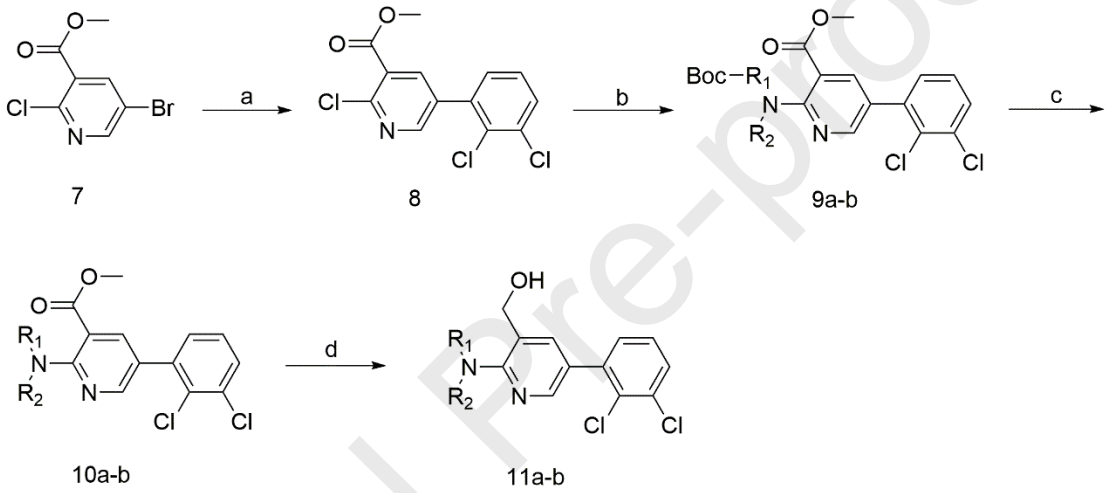

Scheme 2. Synthesis of the target compounds 11a-b. Reagents and condition: (a) $Pd(PPh_3)_4$, Na_2CO_3, 1,4-Dioxane/H_2O, 90°C, 68%; (b) NHR_1R_2Boc, K_2CO_3, DMF, 100°C, 91-92%; (c) TFA, DCM, rt, 91%; (d) $LiAlH_4$, Et_2O, 0°C, 81-82%.

2.2. Biological evaluation

2.2.1. Study on the *in vitro* activity assay of SHP2 and SHP1and structure-activity relationship (SAR)

All the 35 target compounds were used to evaluate the activity of inhibiting phosphatase by using full length wild-type SHP2 and SHP1. The activity results of the target compounds 6a1-6g2 and 11a-b were shown in Table 1. The structure-activity relationship (SAR) was explored below.

Firstly, the SAR on scaffold B was explored. As shown in Table 1, the different substituents on the phenyl ring on the scaffold B had great influence on the activity. When the phenyl ring was a single substituent, the activity at the 2-position substitution was significantly higher than at the 3-position and 4-position substitutions (6a1, 6b1 and 6c1). By comparing the different 2-position substituents, it was found that the activities of Cl, F and CF_3 substituents were significantly higher than that of other substituents (6a1, 6d1-6g1), probably due to the stronger interaction of these substituents with surrounding residues. Subsequently, comparing the activity of two substituents on the phenyl ring, it was found that the activity of the 2,3-position substitution was significantly higher than that of

the 2,4-position and 3,4-position substitutions (6k1-6p1). It is noteworthy that, from the results of the activities of the compounds 6h1 and 6i1, it was found that the substitution of the phenyl ring on the scaffold B for the pyridine ring was advantageous for enhancing the inhibitory activity, and the activity of 6j1 was increased by about 1.7-fold compared with the 6a1.Next, we turned our attention to scaffold C and analyzed the effect of different fragments on activity. When the scaffold C was the aromatic amine group, from the results of the activity of 6c2 and 6f2, the activity of 3-position amino substitution was higher than that of 4-position amino substitution, with an increase of about 1.9-fold. When the scaffold C was the aliphatic amine group, different structures cause significant differences in activity. The difference in activity between compounds 6v1 and 6w1 indicated that the chain length of the extended terminal NH_2 had a significant improvement in activity, resulting in an about 4.3-fold increase in potency of compound 6w1. By comparing the activity results of the compounds 6v1 and 6z1, it was found that the activity of compound 6z1 was increased by about 4.5-fold after the introduction of the methyl group at the terminal of the piperidine, due to the introduction of the methyl group to stabilize the pseudo-equatorial amine conformation. Finally, we turned our attention to skeleton A. The difference in activity was investigated by changing the amino group on the pyridine ring to the hydroxymethyl group. As could be seen from the activity results of compounds 11a and 6w1, after the amino group was changed to the hydroxymethyl group, the compound 11a also had a higher inhibitory activity, and the activity was improved by about 1.2-fold. One reason for the increased activity of compound 11a was that the hydroxymethyl group itself had the function of H bond donor, and another important reason was that the hydroxymethyl group might better match the protein cavity than the amino group. According to the activity results in Table 1, compound 11a (IC_{50} = 1.36 μM) was found to have the best inhibitory activity against SHP2 protein.

Since SHP1 and SHP2 had 60% overall primary sequence identity and about 75% similarity in the catalytic PTP domain, SHP1 and SHP2 proteins exhibited high homology of the protein sequence[26]. Therefore, inhibitors tended to have low selectivity for these two phosphatases. All compounds were tested for their inhibitory activity against SHP1 to assess their selectivity. It could be seen from the table 1 that all compounds exhibited the IC_{50} values of more than 50 μM for SHP1 protein, indicating that these compounds had high selectivity for the SHP2 protein.

Table 1. The SAR studies of the target compounds 6a1-6g2 and 11a-b.

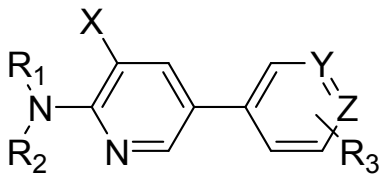

Compd.	X	Y	Z	NR_1R_2	R_3	IC_{50}[a] (μM)	
						SHP2	SHP1
6a1	NH_2	C	C	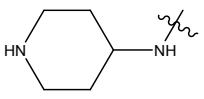	2-Cl	52.12	>100
6b1	NH_2	C	C	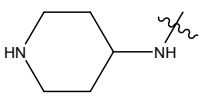	3-Cl	>100	>100

6c1	NH_2	C	C	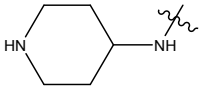	4-Cl	>100	>100
6d1	NH_2	C	C	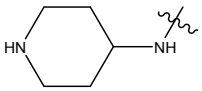	2-F	55.73	>100
6e1	NH_2	C	C	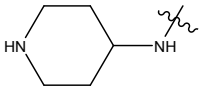	2-OCH_3	>100	>100
6f1	NH_2	C	C	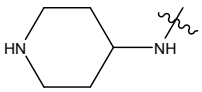	2-CH_3	>100	>100
6g1	NH_2	C	C	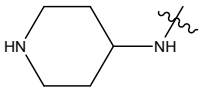	2-CF_3	30.18	>100
6h1	NH_2	N	C	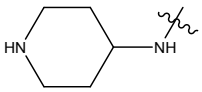	H	8.95	72.54
6i1	NH_2	C	N	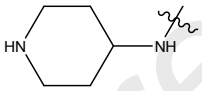	H	34.61	75.43
6j1	NH_2	N	C		2-Cl	30.14	87.61
6k1	NH_2	C	C	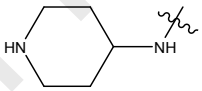	2,3-Cl	28.93	>100
6l1	NH_2	C	C	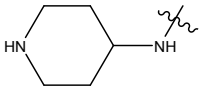	2,4-Cl	85.88	>100
6m1	NH_2	C	C	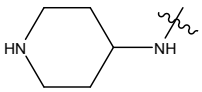	3,4-Cl	>100	>100
6n1	NH_2	C	C	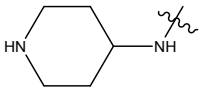	2-Cl-4-CH_3	>100	>100
6o1	NH_2	C	C	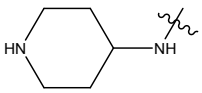	2,3-F	45.66	>100
6p1	NH_2	C	C	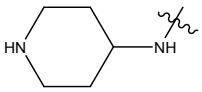	2,4-F	80.39	>100

6q1	NH_2	C	C	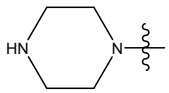	2,3-Cl	33.92	>100
6r1	NH_2	C	C	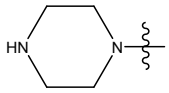	2,3-F	35.74	>100
6s1	NH_2	C	C	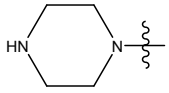	2-Cl	49.36	>100
6t1	NH_2	C	C	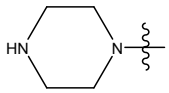	2-CF_3	34.33	>100
6u1	NH_2	C	C	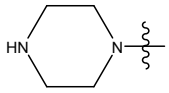	3,4-Cl	>100	>100
6v1	NH_2	C	C	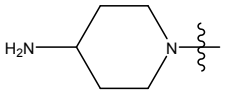	2,3-Cl	7.12	>100
6w1	NH_2	C	C	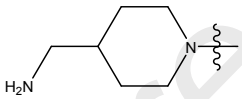	2,3-Cl	1.64	>100
6x1	NH_2	N	C		H	20.73	>100
6y1	NH_2	C	C	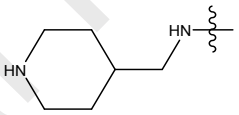	2,3-Cl	27.68	>100
6z1	NH_2	C	C	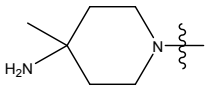	2,3-Cl	1.58	>100
6a2	NH_2	C	C	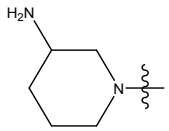	2,3-Cl	16.13	>100
6b2	NH_2	C	C	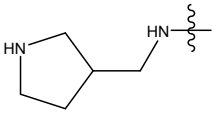	2,3-Cl	24.18	>100
6c2	NH_2	C	C	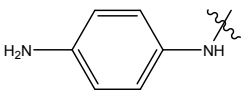	2,3-Cl	18.24	87.24
6d2	NH_2	C	C	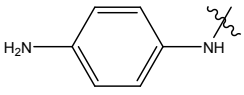	2-Cl	30.60	71.62

6e2	NH2	C	C	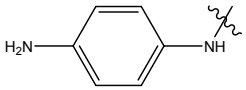	3,4-Cl	>100	62.85
6f2	NH_2	C	C	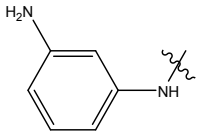	2,3-Cl	9.47	71.28
6g2	NH_2	C	C	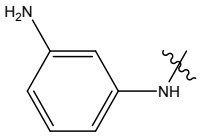	2,3-F	12.31	72.75
11a	CH_2OH	C	C	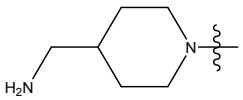	2,3-Cl	1.36	>100
11b	CH_2OH	C	C	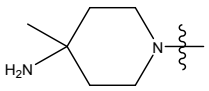	2,3-Cl	1.41	>100
SHP099[b]	—	—	—	—	—	1.48	>100

[a]The experiment was repeated three times and data presented is the mean ±SEM of triplicates from one representative experiment.

[b]Positive control

2.2.2. fluorescence quenching assay

To further verify whether the compound bound directly to SHP2, we performed fluorescence quenching assays on compounds 11a with the best inhibitory activity. As shown in Figure 3, compound 11a showed strong fluorescence quenching of SHP2 protein, respectively, in a dose-dependent manner, indicating that compound 11a would bind directly to SHP2 protein.

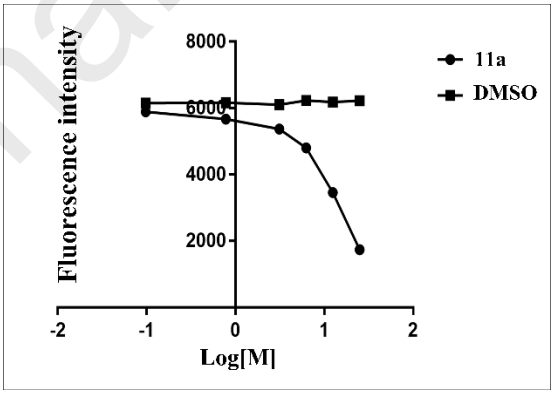

Figure 3. The fluorescence titration of SHP2 protein was carried out by increasing the concentration of compound 11a without changing the concentration of SHP2. The experiment was repeated three times and data presented is the mean ±SEM of triplicates from one representative experiment.

2.2.3. Cell proliferation assay

Cell assay was performed on representative compounds to assess their antiproliferative activity against the Ba/F3 cell line. First, the *in vitro* concentration of the cytotoxicity of the tested compounds was set at 20 μM. Subsequently, these compounds were further assessed to determine their IC_{50} values at concentrations of 0.1, 1.0, 5.0, 10 and 20 μM. Finally, IC_{50} values were calculated.

Table 2 showed the cellular activities of these compounds against the Ba/F_3 cell line. It was found that the tested compounds showed better potency in inhibiting cell proliferation compared to the positive control SHP099. Among them, the compound 11a showed the high activity for inhibiting cell proliferation with an IC_{50} value of 2.35 μM, which was 8.45-fold stronger than SHP099.

Table 2. The antiproliferation IC_{50} values of representative compounds against Ba/F_3 cell.

Compd.	antiproliferation IC_{50}[a] (μM)
6h1	6.62
6v1	6.92
6w1	2.49
6z1	2.32
6f2	7.57
11a	2.35
11b	2.42
SHP099[b]	19.86

[a]The experiment was repeated three times and data presented is the mean ±SEM of triplicates from one representative experiment.

[b]Positive control

2.3. ADMET Prediction

The *in silico* ADMET prediction was used to evaluate the pharmacokinetic properties of these 35 compounds by using DS v3.5 software[27-29]. Discovery Studio 3.5 (DS 3.5) was used to define the prediction level for all ADMET properties. ADMET-Plot was a 2D plot obtained by calculating the PSA_2D and A logp98 features for predicting human intestinal absorption (HIA) and blood-brain barrier (BBB) of all compounds, including 95% and 99% confidence ellipse. As shown in Figure 4, all 35 compounds were within the 99% confidence ellipse, indicating that the target compounds had good human intestinal absorption and could penetrate the blood brain barrier. Based on the structure of the compounds, the parameters of ADMET were calculated in Tables S1 and S2. According to the calculated results, these 35 compounds all were confirmed to be drug-like, and had low side effects.

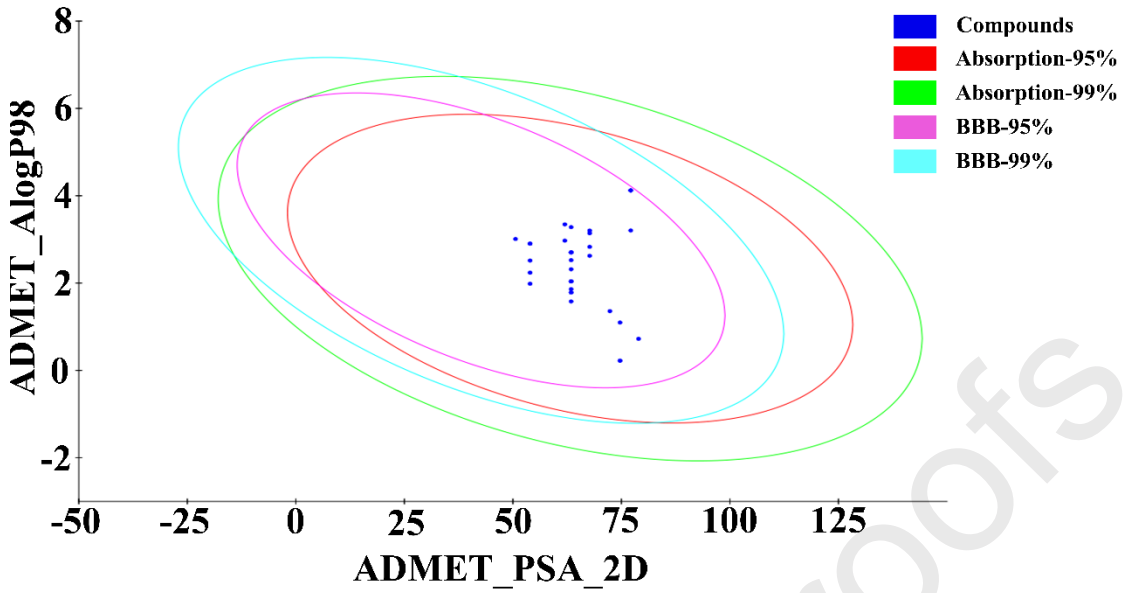

Figure 4. Human intestinal absorption (HIA) and Blood Brain Barrier (BBB) plot of compounds 6a1-g2 and 11a-b. All the compounds in the figure are located in the innermost ellipse, showing better parameter values.

2.4. Molecular docking study

Molecular docking, as an effective and reliable method, can be used to simulate the binding mode between protein and ligand and to understand the protein-inhibitor interaction[30, 31]. As shown in Figures 5A and 5C, with the help of DS v3.5 software, the compounds 6w1 and 11a with higher inhibition potency were docked well in the allosteric binding pocket of SHP2 protein. Here, the docking scores of compounds 6w1 and 11a were 56.24 and 58.62, respectively. To further explore the interaction of compounds 6w1 and 11a with SHP2, the docking result was visualized as 2D diagram, as shown in Figures 5B and 5D, which clearly showed the interaction of compounds 6w1 and 11a with SHP2 protein. It was found that compound 6w1 formed H bond interactions with residues Thr108, Glu110, Arg111, Phe113 and His114 between the C-SH2 and N-SH2 domains and residues Leu216, Thr218 and Thr253 of the PTP domain. And compound 11a formed H bond interactions with residues Thr108, Glu110, Arg111 and Phe113 between the C-SH2 and N-SH2 domains and residues Thr218, Thr219 and Thr253 of the PTP domain. And the dichlorophenyl groups in both compounds formed hydrophobic interactions with the surrounding residues, and both formed cation-Pi interactions with the key residue Arg111. Therefore, both compounds formed stable interactions with SHP2 protein, which revealed at the molecular level why both compounds had High inhibitory activity.

The structural differences of compounds 6w1, 11a and SHP099 were mainly in the mother nucleus. It had been reported that on the aminopyrazine ring of SHP099, the amino group mainly formed an H bond interaction with the residue Glu250. On the aminopyridine ring of compound 6w1, the amino group formed three H bond interactions with residues His114, Leu216, and Thr218. On the hydroxymethylpyridine ring of compound 11a, the hydroxymethyl group formed three H bond interactions with the residues Thr218 and Thr219. Therefore, pyridine derivatives could effectively match with protein pocket and formed stable interactions, thus exhibiting higher inhibitory activity. In addition, we further analyzed the difference in H bond distance and found that the H bond formed by compound 11a was more stable than that formed by compound 6w1, which also explained why

the inhibitory activity of compound 11a was slightly higher than that of compound 6w1.

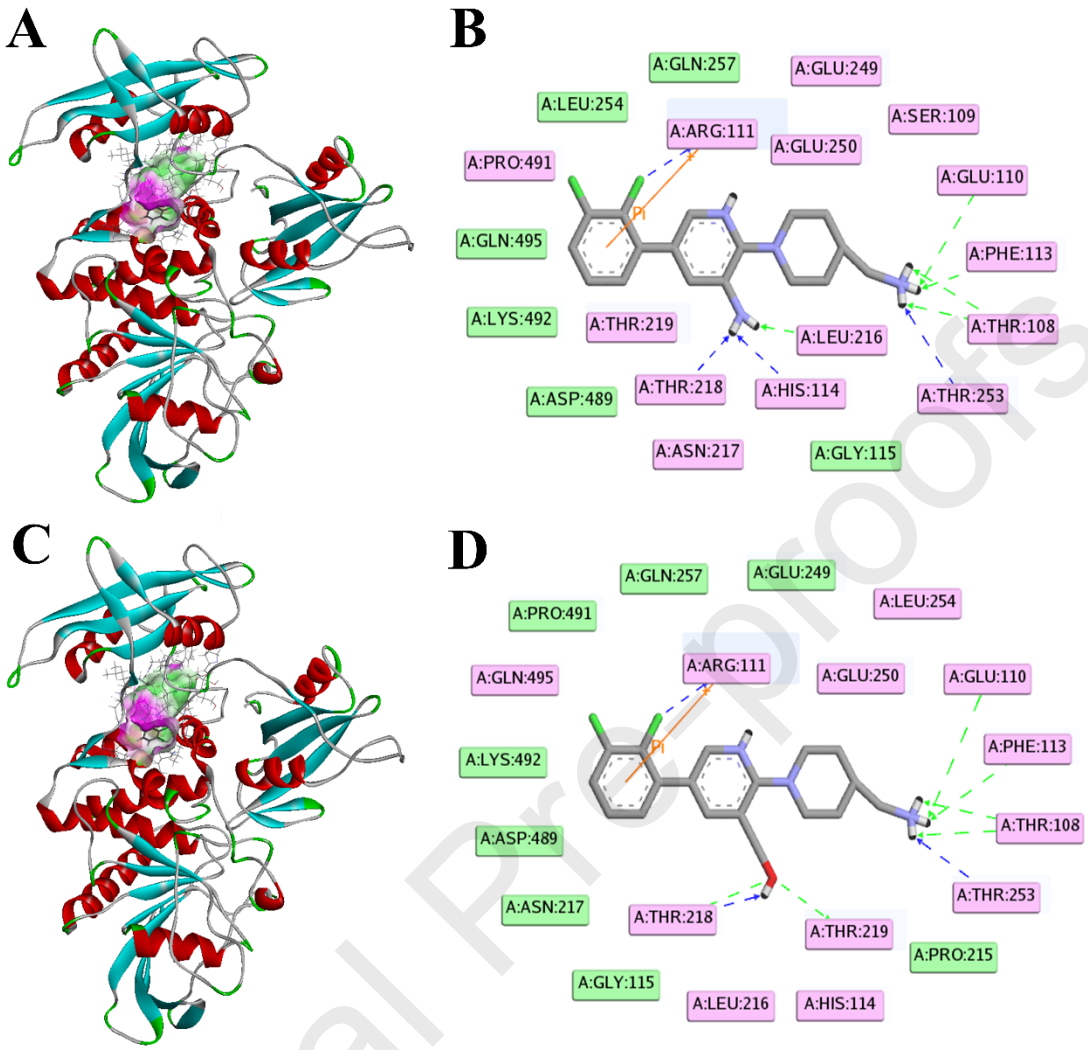

Figure 5. The binding mode of compounds 6w1 and11a with SHP2 protein. (A) The docking pocket of compound 6w1 and SHP2. (B) 2D diagram of the interaction of compound 6w1 and SHP2 protein. (C) The docking pocket of compound 11a and SHP2. (D) 2D diagram of the interaction of compound 11a and SHP2 protein. Among them, the H bond interactions with residues are denoted by green dotted arrow pointing to the electron donor; the H bond interactions with residues are denote d by blue dashed arrow pointing to the electron donor; the cation-Pi interactions are represented by the orange line; the pink rectangles represent residues with charge or H bond interactions; the green rectangles represent residues with VDW interactions.

3. Conclusion

SHP2 has attracted extensive attention as an anticancer target due to its direct correlation with cancer and its influence on the transduction of various signaling pathways. Therefore, the development of SHP2 small molecule inhibitors is particularly urgent. In this study, based on the inhibitor SHP099, 35 novel SHP2 inhibitors with 3-substituted pyridine as the core structure were designed by means of scaffold hopping. Subsequently, analysis of the *in vitro* enzyme activity assay gained a number of inhibitors with the exploitable value. Among them, the compound 11a was the most potent SHP2 inhibitor and its *in vitro* enzyme activity IC_{50} value reached 1.36 μM, and the activity against SHP1 exceeded 100 μM, showing high selectivity for SHP2 protein. Fluorescence quenching assay

verified that compound 11a bound directly to the SHP2 protein. The cell activity studies of representative compounds found that the tested compounds all showed effective antiproliferative activity on Ba / F3 cells, of which the IC_{50} value of 11a was 2.35 μM. Furthermore, the *in silico* ADMET prediction validated that these compounds were potential to be drug-like. The binding modes of the compound 11a and 6w1 with SHP2 protein were explored by the molecular docking, and the reason for the difference in activity between the two compounds was explored at the molecular level. It was found that the H bond interaction formed between the hydroxymethyl group and protein was more stable, revealing that the inhibitory activity of compound 11a was slightly higher than that of the compound 6w1. In summary, through our series of studies, we sincerely hope that this research can provide more new ideas for the development of more effective SHP2 inhibitors.

4. Experimental section

4.1. Chemistry

Reagents and solvents were obtained from commercial suppliers and could be used directly without further purification. Analytical thin layer chromatography (TLC) was performed on the TLC plate (silica gel 60 F254 and aluminum foil). All compounds were detected by using UV light (wavelength: 254 nm or 365 nm). The Isolation and purification of compound was carried out by flash column chromatography on silica gel 60 (300-400 mesh). ^{1}H (400 MHz) and ^{13}C NMR (100 MHz) spectra were recorded in $CDCl_3$ or DMSO-d_6 by the spectrometer at room temperature. Chemical shifts were reported in parts per million (ppm) and coupling constants (*J*) were expressed in Hz. The characteristics of the signal were s (singlet), d (doublet), dd (doublet of doublets), t (triplet) and m (multiplet). Mass spectra were measured on an Agilent 1100 series.

4.1.1. General procedure for the synthesis of 3a-j, 4a1-g2, 5a1-g2, 6a1-g2, 8, 9a-b, 10a-b and 11a-b.

A mixture of 5-Bromo-2chloro-3-nitropyridine (2) (10 mmol), organicamine compound (14 mmol), and N,N-diisopropylethylamine (30 mmol) in 1,4-dioxane (100 mL) was stirred at room temperature for 4 h. After the reaction was completed by TLC analysis, the volatiles were removed under reduced pressure. The mixture was extracted with CH_2Cl_2 (3 × 60 mL) and washed with H_2O (3 × 60 mL). The combined organic layers were dried over anhydrous Na_2SO_4 and concentrated in vacuo. The resulting residue was purified by column chromatography on silica gel (PE: EA = 9:1) to obtain the intermediates 3a-j.

A suspension of intermediate 3a-j (2 mmol), boric acid compound (3 mmol), $Pd(PPh_3)_4$ (0.16 mmol) and K_2CO_3 (6 mmol) in 1,4-dioxane/H_2O (5:1, 60 mL) was heated to 120 °C and stirred for 6 h. After completion of the reaction by TLC analysis, the solvent was removed in vacuo. The mixture was extracted with CH_2Cl_2 (3 × 40 mL) and washed with H_2O (3 × 40 mL). The organic phases were combined and dried over anhydrous Na_2SO_4. The organic phase after drying was evaporated under reduced pressure, and the resulting residue obtained was purified by silica gel chromatography on silica gel (PE: EA = 6:1) to gain the intermediates 4a1-g2.

The mixture of the intermediate 4a1-g2 (1.3mmol), zinc powder (26 mmol) and ammonium chloride (6.5 mmol) in EtOH/H_2O (10:1, 55mL) was heated to 80 °C and stirred for 6 h. After the reaction was completed, the iron powder was removed by suction filtration, and then the volatiles were removed in vacuo. PH of the mixture was basified to 9 with saturated $NaHCO_3$ solution, then

extracted with EtOAc (3 × 30 mL) and washed with saturated brine (3 × 30 mL). The organic phases were combined and dried over anhydrous Na_2SO_4. The dried organic phase was decompressed to remove the solvent, and the obtained residue was purified by silica gel chromatography on silica gel (PE: EA = 3:1) to obtain the intermediates 5a1-g2.

The mixture of intermediates 5a1-g2 (0.9mmol) and trifluoroacetic acid (18mmol) in dichloromethane (15mL) was stirred at room temperature for 20 minutes, and the reaction was completed by TLC analysis. The volatiles were removed under reduced pressure and the residue obtained was diluted with CH_2Cl_2 (10mL) and H_2O (10mL). The phases were separated and the aqueous phase was further extracted with CH_2Cl_2 (2 × 5 mL). The combined organic phases were discarded and the aqueous phase was basified to pH 10 with saturated Na_2CO_3 and extracted with EtOAc (3 × 10 mL). The combined organic phases were dried over anhydrous Na_2SO_4, and the solvent was removed under reduced pressure to obtain the final products 6a1-g2.

A suspension of methyl 5-bromo-2-chloronicotinate (7) (8 mmol), (2,3-dichlorophenyl)boronic acid (12 mmol), $Pd(PPh_3)_4$ (0.64 mmol) and Na_2CO_3 (24 mmol) in 1,4-dioxane/H_2O (9:1, 80 mL) was heated to 90 °C and stirred for 3 h. After the reaction was completed, the solvent was removed in vacuo. The mixture was extracted with CH_2Cl_2 (3 × 50 mL) and washed with H_2O (3 × 50 mL). The organic phases were combined and dried over anhydrous Na_2SO_4. The organic phase after drying was evaporated under reduced pressure, and the resulting residue obtained was purified by silica gel chromatography on silica gel (PE: EA = 8:1) to gain the intermediate 8.

A mixture of intermediate 8 (4 mmol), organicamine compound (6 mmol), and K_2CO_3 (12 mmol) in DMF (60 mL) was heated to 100 °C for 4 h. After the reaction was completed by TLC analysis, the volatiles were removed under reduced pressure. The mixture was extracted with CH_2Cl_2 (3 × 40 mL) and washed with H_2O (3 × 40 mL). The combined organic layers were dried over anhydrous Na_2SO_4 and concentrated in vacuo. The resulting residue was purified by column chromatography on silica gel (PE: EA = 5:1) to obtain the intermediates 9a-b.

The mixture of intermediates 9a-b (2 mmol) and trifluoroacetic acid (40 mmol) in dichloromethane (40 mL) was stirred at room temperature for 20 minutes, and the reaction was completed by TLC analysis. The volatiles were removed under reduced pressure and the residue obtained was diluted with CH_2Cl_2 (20 mL) and H_2O (20 mL). The phases were separated and the aqueous phase was further extracted with CH_2Cl_2 (2 × 10 mL). The combined organic phases were discarded and the aqueous phase was basified to pH 10 with saturated Na_2CO_3 and extracted with EtOAc (3 × 20 mL). The combined organic phases were dried over anhydrous Na_2SO_4, and the solvent was removed under reduced pressure to obtain the intermediates 10a-b.

A suspension of 10a-b (0.8 mmol) in Et_2O (25 mL) was stirred in ice bath for 5 minutes. Then, lithium aluminum hydride (8 mmol) was added to the reaction flask, and the reaction was continued for 2 hours. After the reaction was completed, it was quenched by adding 15% sodium hydroxide solution. The insoluble matter was then removed by filtration. The mixture was extracted with CH_2Cl_2 (3 × 30 mL) and washed with H_2O (3 × 20 mL). Organic phases were combined and dried with anhydrous Na_2SO_4. The dried organic phase was evaporated under reduced pressure and the residue obtained was purified by silica gel chromatography (CH_2Cl_2: MeOH = 10:1, 0.6% ammonium hydroxide) to obtain the final products 11a-b.

4.1.1.1. 5-(2-chlorophenyl)-N^2-(piperidin-4-yl)pyridine-2,3-diamine (6a1)

White solid, yield 89%, mp 167-169 °C, ^{1}H NMR (400 MHz, DMSO-d_6): δ 7.49 (d, J = 8.0 Hz, 1H),

7.41 (d, J = 2.0 Hz, 1H), 7.28-7.37 (m, 3H), 6.80 (d, J = 2.0 Hz, 1H), 5.54 (d, J = 7.2 Hz, 1H), 4.90 (s, 2H), 3.90-4.02 (m, 1H), 2.98 (d, 2H), 2.84 (s, 1H), 2.56 (t, 2H), 1.92 (d, 2H), 1.28-1.39 (m, 2H); ^{13}C NMR (100 MHz, DMSO-d_6) δ 146.3, 138.2, 134.6, 131.6, 131.2, 129.8, 129.2, 128.2, 127.3, 123.0, 118.2, 47.6, 45.1 (2C), 33.1 (2C); MS (m/z): 303.1 $[M + H]^+$.

4.1.1.2. 5-(3-chlorophenyl)-N^2-(piperidin-4-yl)pyridine-2,3-diamine (6b1)
White solid, yield 88%, mp 161-163 °C, ^{1}H NMR (400 MHz, DMSO-d_6): δ 7.73 (d, J = 2.0 Hz, 1H), 7.51 (s, 1H), 7.46 (d, J = 8.0 Hz, 1H), 7.40 (t, 1H), 7.29 (d, J = 8.0 Hz, 1H), 6.99 (d, J = 2.0 Hz, 1H), 5.61 (d, J = 7.2 Hz, 1H), 4.91 (s, 2H), 3.90-4.02 (m, 1H), 2.97 (d, 2H), 2.55 (t, 3H), 1.89 (d, 2H), 1.25-1.38 (m, 2H); ^{13}C NMR (100 MHz, DMSO-d_6) δ 146.9, 141.2, 133.5, 133.0, 130.6, 130.1, 125.6, 124.8, 123.8, 122.6, 115.2, 48.0, 45.3 (2C), 33.5 (2C); MS (m/z): 303.1 $[M + H]^+$.

4.1.1.3. 5-(4-chlorophenyl)-N^2-(piperidin-4-yl)pyridine-2,3-diamine (6c1)
White solid, yield 87%, mp 164-166 °C, ^{1}H NMR (400 MHz, DMSO-d_6): δ 7.71 (d, J = 2.0 Hz, 1H), 7.51 (d, J = 8.4 Hz, 2H), 7.42 (d, J = 8.4 Hz, 2H), 6.97 (d, J = 2.0 Hz, 1H), 5.56 (d, J = 7.2 Hz, 1H), 4.93 (s, 2H), 3.90-4.02 (m, 1H), 2.98 (d, 2H), 2.52-2.70 (m, 3H), 1.91 (d, 2H), 1.24-1.41 (m, 2H); ^{13}C NMR (100 MHz, DMSO-d_6) δ 146.7, 137.8, 132.8, 130.5, 130.1, 128.7 (2C), 126.9 (2C), 122.9, 115.1, 48.0, 45.4 (2C), 33.6 (2C); MS (m/z): 303.1 $[M + H]^+$.

4.1.1.4. 5-(2-fluorophenyl)-N^2-(piperidin-4-yl)pyridine-2,3-diamine (6d1)
White solid, yield 91%, mp 167-169 °C, ^{1}H NMR (400 MHz, DMSO-d_6): δ 7.56 (s, 1H), 7.41 (t, 1H), 7.26-7.33 (m, 1H), 7.19-7.26 (m, 2H), 6.90 (s, 1H), 5.58 (d, J = 7.2 Hz, 1H), 4.92 (s, 2H), 3.90-4.02 (m, 1H), 2.99 (d, 3H), 2.57 (t, 2H), 1.92 (d, 2H), 1.28-1.41 (m, 2H); ^{13}C NMR (100 MHz, DMSO-d_6) δ 159.1 (d, J = 243.1 Hz), 146.5, 134.5 (d, J = 3.6 Hz), 129.8 (d, J = 3.8 Hz), 129.7, 128.1 (d, J = 8.1 Hz), 126.8 (d, J = 13.3 Hz), 124.8 (d, J = 3.3 Hz), 119.2 (J = 1.2 Hz), 117.4 (J = 3.0 Hz), 115.9 (d, J = 22.6 Hz), 47.7, 45.1 (2C), 33.2 (2C); MS (m/z): 287.2 $[M + H]^+$.

4.1.1.5. 5-(2-methoxyphenyl)-N^2-(piperidin-4-yl)pyridine-2,3-diamine (6e1)
White solid, yield 90%, mp 165-167 °C, ^{1}H NMR (400 MHz, DMSO-d_6): δ 7.47 (d, J = 2.0 Hz, 1H), 7.24 (t, 1H), 7.19 ((dd, J = 1.6 Hz, J = 7.2 Hz, 1H), 7.04 (d, J = 8.0 Hz, 1H), 6.96 (t, 1H), 6.87 (d, J = 2.0 Hz, 1H), 5.38 (d, J = 7.2 Hz, 1H), 4.77 (s, 2H), 3.88-4.02 (m, 1H), 3.74 (s, 3H), 2.98 (d, 2H), 2.90 (s, 1H), 2.56 (t, 2H), 1.92 (d, 2H), 1.26-1.39 (m, 2H); ^{13}C NMR (100 MHz, DMSO-d_6) δ 156.2, 146.0, 134.8, 129.6, 129.0, 128.3, 127.7, 122.3, 120.6, 118.9, 111.5, 55.3, 47.8, 45.3 (2C), 33.5 (2C); MS (m/z): 299.2 $[M + H]^+$.

4.1.1.6. N^2-(piperidin-4-yl)-5-(*o*-tolyl)pyridine-2,3-diamine (6f1)
White solid, yield 89%, mp 161-163 °C, ^{1}H NMR (400 MHz, DMSO-d_6): δ 7.33 (s, 1H), 7.09-7.27 (m, 4H), 6.70 (s, 1H), 5.43 (d, J = 7.2 Hz, 1H), 4.84 (s, 2H), 3.88-4.02 (m, 1H), 2.98 (d, 2H), 2.67 (s, 1H), 2.56 (t, 2H), 2.25 (s, 3H), 1.93 (d, 2H), 1.26-1.40 (m, 2H); ^{13}C NMR (100 MHz, DMSO-d_6) δ 145.9, 139.5, 134.9, 134.4, 130.2, 129.4, 129.3, 126.5, 125.8, 125.2, 118.4, 47.9, 45.4 (2C), 33.6 (2C), 20.4; MS (m/z): 283.2 $[M + H]^+$.

4.1.1.7. N^2-(piperidin-4-yl)-5-(2-(trifluoromethyl)phenyl)pyridine-2,3-diamine (6g1)
White solid, yield 91%, mp 169-171 °C, ^{1}H NMR (400 MHz, DMSO-d_6): δ 7.77 (d, J = 7.6 Hz, 1H),

7.66 (t, 1H), 7.53 (t, 1H), 7.37 (d, *J* = 7.6 Hz, 1H), 7.29 (d, *J* = 1.6 Hz, 1H), 6.67 (d, *J* = 1.6 Hz, 1H), 5.50 (d, *J* = 7.2 Hz, 1H), 4.91 (s, 2H), 3.86-4.03 (m, 3H), 2.97 (d, 2H), 2.56 (t, 2H), 1.91 (d, 2H), 1.26-1.40 (m, 2H); ^{13}C NMR (100 MHz, DMSO-d_6) δ 146.4, 139.3 (d, *J* = 1.9 Hz), 133.9, 132.5, 132.1, 129.0, 127.2, 126.9, 125.9, 124.3 (d, *J* = 272.3 Hz), 123.5, 117.9, 47.9, 45.3 (2C), 33.5 (2C); MS (m/z): 337.2 $[M + H]^+$.

4.1.1.8. N^6-(piperidin-4-yl)-[3,3'-bipyridine]-5,6-diamine (6h1)
Pale yellow solid, yield 91%, mp 171-173 °C, ^{1}H NMR (400 MHz, DMSO-d_6): δ 8.75 (d, *J* = 2.0 Hz, 1H), 8.44-8.48 (m, 1H), 7.88 (d, *J* = 8.0 Hz, 1H), 7.77 (d, *J* = 2.0 Hz, 1H), 7.37-8.44 (m, 1H), 7.02 (d, *J* = 2.0 Hz, 1H), 5.65 (d, *J* = 7.2 Hz, 1H), 4.99 (d, 2H), 3.89-4.06 (m, 1H), 2.95-3.05 (m, 2H), 2.80 (s, 1H), 2.53-2.63 (m, 2H), 1.88-2.00 (m, 2H), 1.27-1.43 (m, 2H); ^{13}C NMR (100 MHz, DMSO-d_6) δ 147.0, 146.9, 146.4, 134.4, 133.0, 132.5, 130.3, 123.7, 121.0, 115.0, 48.0, 45.4 (2C), 33.5 (2C); MS (m/z): 270.2 $[M + H]^+$.

4.1.1.9. N^6-(piperidin-4-yl)-[3,4'-bipyridine]-5,6-diamine (6i1)
Pale yellow solid, yield 89%, mp 163-165 °C, ^{1}H NMR (400 MHz, DMSO-d_6): δ 8.49-8.54 (m, 2H), 7.91 (d, *J* = 2.0 Hz, 1H), 7.51-7.55 (m, 2H), 7.10 (d, *J* = 2.0 Hz, 1H), 5.85 (d, *J* = 7.2 Hz, 1H), 5.04 (s, 2H), 3.99-4.09 (m, 1H), 3.79-3.98 (s, 3H), 3.02-3.12 (m, 2H), 2.61-2.73 (m, 2H), 1.92-2.01 (m, 2H), 1.35-1.48 (m, 2H); 13C NMR (101 MHz, DMSO) δ 149.9 (2C), 147.6, 145.8, 133.5, 130.3, 120.8, 119.5 (2C), 114.4, 47.9, 44.7 (2C), 32.4 (2C); MS (m/z): 270.2 $[M + H]^+$.

4.1.1.10. 2'-chloro-N^6-(piperidin-4-yl)-[3,3'-bipyridine]-5,6-diamine (6j1)
White solid, yield 92%, mp 166-168 °C, ^{1}H NMR (400 MHz, DMSO-d_6): δ 8.34 (dd, *J* = 2.0 Hz, *J* = 7.6 Hz, 1H), 7.79 (dd, *J* = 2.0 Hz, *J* = 7.6 Hz, 1H), 7.42-7.48 (m, 2H), 6.83 (d, *J* = 2.0 Hz, 1H), 5.63 (d, *J* = 7.2 Hz, 1H), 4.96 (s, 2H), 3.91-4.03 (m, 1H), 2.98 (d, 2H), 2.56 (t, 3H), 1.82 (d, 2H), 1.26-1.40 (m, 2H); ^{13}C NMR (100 MHz, DMSO-d_6) δ 148.66, 147.6, 146.7, 139.8, 134.8, 134.8, 129.3, 123.4, 121.1, 117.6, 48.0, 45.4 (2C), 33.5 (2C); MS (m/z): 305.2 $[M + H]^+$.

4.1.1.11. 5-(2,3-dichlorophenyl)-N^2-(piperidin-4-yl)pyridine-2,3-diamine (6k1)
White solid, yield 91%, mp 170-172 °C, ^{1}H NMR (400 MHz, DMSO-d_6): δ 7.57 (d, *J* = 7.6 Hz, 1H), 7.40 (d, *J* = 1.6 Hz, 1H), 7.37 (t, 1H), 7.30 (d, *J* = 7.6 Hz, 1H), 6.77 (d, *J* = 1.6 Hz, 1H), 5.59 (d, *J* = 7.2 Hz, 1H), 4.92 (s, 2H), 3.98-4.03 (m, 1H), 2.97 (d, 2H), 2.53 (d, 2H), 2.27 (s, 1H), 1.89 (d, 2H), 1.25-1.39 (m, 2H); ^{13}C NMR (100 MHz, DMSO-d_6): δ 146.6, 140.9, 134.6, 132.2, 129.8 (2C), 129.2, 128.8, 128.1, 122.8, 117.8, 47.9, 45.3, (2C) 33.5 (2C); MS (m/z): 337.1 $[M + H]^+$.

4.1.1.12. 5-(2,4-dichlorophenyl)-N^2-(piperidin-4-yl)pyridine-2,3-diamine (6l1)
White solid, yield 87%, mp 172-174 °C, ^{1}H NMR (400 MHz, DMSO-d_6): δ 7.65 (d, *J* = 2.4 Hz, 1H), 7.44 (dd, *J* = 2.0 Hz, *J* = 8.0 Hz, 1H), 7.40 (d, *J* = 2.0 Hz, 1H), 7.34 (d, *J* = 8.4 Hz, 1H), 6.77 (d, *J* = 2.4 Hz, 1H), 5.58 (d, *J* = 7.2 Hz, 1H), 4.92 (s, 2H), 3.89-4.01 (m, 1H), 2.96 (d, 2H), 2.54 (d, 2H), 2.28 (s, 1H), 1.90 (d, 2H), 1.25-1.37 (m, 2H); ^{13}C NMR (100 MHz, DMSO-d_6) δ 146.5, 137.3, 134.7, 132.5, 132.3, 131.8, 129.2, 129.1, 127.5, 121.8, 117.8, 48.0, 45.4 (2C), 33.6 (2C); MS (m/z): 337.1 $[M + H]^+$.

4.1.1.13. 5-(3,4-dichlorophenyl)-N^2-(piperidin-4-yl)pyridine-2,3-diamine (6ml)

White solid, yield 89%, mp 160-162 °C, ^{1}H NMR (400 MHz, DMSO-d_6): δ 7.75 (s, 1H), 7.71 (s, 1H), 7.61 (d, J = 7.6 Hz, 1H), 7.49 (d, J = 7.6 Hz, 1H), 6.99 (s, 1H), 5.65 (d, J = 7.2 Hz, 1H), 4.93 (s, 2H), 3.90-4.02 (m, 1H), 2.98 (d, 2H), 2.56 (d, 2H), 1.90 (d, 2H), 1.25-1.40 (m, 2H), 1.22 (s, 1H); ^{13}C NMR (100 MHz, DMSO-d_6) δ 147.0, 139.7, 133.1, 131.5, 130.8, 130.1, 128.2, 126.7, 125.3, 121.5, 114.9, 48.0, 45.3 (2C), 33.4 (2C); MS (m/z): 337.1 $[M + H]^+$.

4.1.1.14. 5-(2-chloro-4-methylphenyl)-N^2-(piperidin-4-yl)pyridine-2,3-diamine (6nl)
White solid, yield 90%, mp 161-163 °C, ^{1}H NMR (400 MHz, DMSO-d_6): δ 7.39 (d, J = 2.0 Hz, 1H), 7.33 (s, 1H), 7.20 (d, J = 7.6 Hz, 1H), 7.16 (d, J = 7.6 Hz, 1H), 6.78 (d, J = 2.0 Hz, 1H), 5.51 (d, J = 7.2 Hz, 1H), 4.88 (s, 2H), 3.88-4.02 (m, 1H), 2.98 (d, 2H), 2.74 (s, 1H), 2.55 (t, 2H), 2.31 (s, 3H), 1.90 (d, 2H), 1.26-1.40 (m, 2H); ^{13}C NMR (100 MHz, DMSO-d_6) δ 146.2, 137.9, 135.3, 134.6, 131.2, 130.9, 130.0, 129.1, 128.0, 122.9, 118.3, 47.9, 45.4 (2C), 33.6 (2C), 20.2; MS (m/z): 317.2 $[M + H]^+$.

4.1.1.15. 5-(2,3-difluorophenyl)-N^2-(piperidin-4-yl)pyridine-2,3-diamine (6o1)
White solid, yield 89%, mp 166-168 °C, ^{1}H NMR (400 MHz, DMSO-d_6): δ 7.60 (s, 1H), 7.28-7.35 (m, 1H), 7.19 -7.27 (m, 2H), 6.92 (s, 1H), 5.68 (d, J = 7.2 Hz, 1H), 4.98 (s, 2H), 3.92-4.06 (m, 1H), 3.52 (s, 1H), 3.02 (d, 2H), 2.61 (t, 2H), 1.94 (d, 2H), 1.28-1.45 (m, 2H); ^{13}C NMR (100 MHz, DMSO-d_6): δ 150.3 (dd, J = 13.4 Hz, J = 243.3 Hz), 146.9 (dd, J = 12.8 Hz, J = 244.5 Hz), 146.8, 134.6 (d, J = 3.8 Hz), 129.8, 129.2 (d, J = 10.0 Hz), 124.8, 124.7, 118.1, 117.0 (d, J = 2.8 Hz), 114.9 (d, J = 17.1 Hz), 47.7, 45.1 (2C), 33.0 (2C); MS (m/z): 305.2 $[M + H]^+$.

4.1.1.16. 5-(2,4-difluorophenyl)-N^2-(piperidin-4-yl)pyridine-2,3-diamine (6p1)
White solid, yield 91%, mp 164-166 °C, ^{1}H NMR (400 MHz, DMSO-d_6): δ 7.52 (s, 1H), 7.40-7.48 (s, 1H), 7.28 (t, 1H), 7.12 (t, 1H), 6.86 (s, 1H), 5.59 (d, J = 7.2 Hz, 1H), 4.93 (s, 2H), 3.90-4.02 (m, 1H), 3.07 (s, 1H), 2.99 (d, 2H), 2.57 (t, 2H), 1.91 (d, 2H), 1.27-1.40 (m, 2H); ^{13}C NMR (100 MHz, DMSO-d_6) δ 160.8 (dd, J = 11.7 Hz, J = 243.3 Hz), 159.0 (dd, J = 12.0 Hz, J = 245.7 Hz), 146.5, 134.3 (d, J = 3.1 Hz), 130.8, 129.7, 123.5 (dd, J = 3.7 Hz, J = 13.7 Hz), 118.4 (d, J = 1.4 Hz), 117.3 (J = 2.8 Hz), 111.9 (dd, J = 3.5 Hz, J = 20.8 Hz), 104.3, 47.7, 45.2 (2C), 33.2 (2C); MS (m/z): 305.2 $[M + H]^+$.

4.1.1.17. 5-(2,3-dichlorophenyl)-2-(piperazin-1-yl)pyridin-3-amine (6q1)
White solid, yield 90%, mp 162-164 °C, ^{1}H NMR (400 MHz, DMSO-d_6): δ 7.65 (d, J = 8.0 Hz, 1H), 7.60 (d, J = 1.6 Hz, 1H), 7.42 (t, 1H), 7.37 (d, J = 8.0 Hz, 1H), 7.03 (d, J = 1.6 Hz, 1H), 4.93 (s, 2H), 2.85-3.01 (m, 9H); ^{13}C NMR (100 MHz, DMSO-d_6) δ 149.9, 140.0, 135.6, 134.7, 132.3, 130.0, 129.9, 129.6, 129.6, 128.3, 120.8, 49.3 (2C), 45.6 (2C); MS (m/z): 323.1 $[M + H]^+$.

4.1.1.18. 5-(2,3-difluorophenyl)-N^2-(piperidin-4-yl)pyridine-2,3-diamine (6r1)
White solid, yield 88%, mp 168-170 °C, ^{1}H NMR (400 MHz, DMSO-d_6): δ 7.76 (s, 1H), 7.37-7.46 (m, 1H), 7.25-7.35 (m, 2H), 7.16 (s, 1H), 4.97 (s, 2H), 2.84-3.05 (m, 9H); ^{13}C NMR (100 MHz, DMSO-d_6) δ 150.2 (dd, J = 13.3 Hz, J = 243.8 Hz), 150.2, 147.0 (dd, J = 12.9 Hz, J = 245.4 Hz), 136.0, 134.6, 128.3 (d, J = 1.6 Hz), 125.3, 125.1, 124.9, 120.2 (d, J = 2.6 Hz), 116.2 (d, J = 17.0 Hz), 49.2 (2C), 45.5 (2C); MS (m/z): 291.1 $[M + H]^+$.

4.3.1.19. 5-(2-chlorophenyl)-2-(piperazin-1-yl)pyridin-3-amine (6s1)
White solid, yield 92%, mp 167-169 °C, ^{1}H NMR (400 MHz, DMSO-d_6): δ 7.60 (d, J = 2.0 Hz, 1H), 7.52-7.57 (m, 1H), 7.36-7.42 (m, 3H), 7.05 (d, J = 2.0 Hz, 1H), 4.93 (s, 2H), 3.24 (s, 1H), 2.95-3.02 (m, 4H), 2.86-2.94 (m, 4H); ^{13}C NMR (100 MHz, DMSO-d_6) δ 149.6, 137.4, 135.6, 134.8, 131.6, 131.4, 129.8 (2C), 129.1, 127.5, 121.1, 49.2 (2C), 45.5 (2C); MS (m/z): 289.1 $[M + H]^+$.

4.1.1.20. 2-(piperazin-1-yl)-5-(2-(trifluoromethyl)phenyl)pyridin-3-amine (6t1)
White solid, yield 90%, mp 162-164 °C, ^{1}H NMR (400 MHz, DMSO-d_6): δ 7.82 (d, J = 7.6 Hz, 1H), 7.71 (t, 1H), 7.60 (t, 1H), 7.50 (d, J = 2.0 Hz, 1H), 7.41 (d, J = 7.6 Hz, 1H), 6.94 (d, J = 2.0 Hz, 1H), 4.94 (s, 2H), 2.85-3.06 (m, 9H); 13C NMR (101 MHz, DMSO) δ 149.7, 138.2 (d, J = 1.9 Hz), 135.4, 134.3, 132.3, 132.2, 130.3, 127.9, 127.1 (d, J = 28.9 Hz), 126.0, 124.2 (d, J = 272.3 Hz), 120.7, 49.2 (2C), 45.6 (2C); MS (m/z): 323.1 $[M + H]^+$.

4.1.1.21. 5-(3,4-dichlorophenyl)-2-(piperazin-1-yl)pyridin-3-amine (6u1)
White solid, yield 87%, mp 165-167 °C, ^{1}H NMR (400 MHz, DMSO-d_6): δ 7.91 (s, 1H), 7.82 (s, 1H), 7.69 (d, d, J = 8.4 Hz, 1H), 7.57 (d, J = 8.4 Hz, 1H), 7.24 (s, 1H), 4.91 (s, 2H), 2.94-3.02 (m, 4H), 2.84-2.92 (m, 4H), 2.68 (s, 1H); 13C NMR (101 MHz, DMSO) δ 150.4, 138.9, 136.3, 133.1, 131.6, 131.0, 129.7, 128.4, 127.8, 126.3, 118.2, 49.2 (2C), 45.5 (2C); MS (m/z): 323.1 $[M + H]^+$.

4.1.1.22. 2-(4-aminopiperidin-1-yl)-5-(2,3-dichlorophenyl)pyridin-3-amine (6v1)
White solid, yield 92%, mp 164-166 °C, ^{1}H NMR (400 MHz, DMSO-d_6): δ 7.65 (dd, J = 1.2 Hz, J = 8.0 Hz, 1H), 7.58 (d, J = 2.0 Hz, 1H), 7.42 (t, 1H), 7.36 (d, J = 7.6 Hz, 1H), 7.02 (d, J = 2.0 Hz, 1H), 4.90 (s, 2H), 3.39 (d, 2H), 2.62-2.75 (m, 3H), 1.80 (d, 2H), 1.69 (s, 2H), 1.37-1.50 (m, 2H); ^{13}C NMR (100 MHz, DMSO-d_6) δ 150.1, 140.0, 135.6, 134.7, 132.3, 130.0, 129.9, 129.6, 129.5, 128.3, 120.7, 48.5, 47.2 (2C), 35.5 (2C); MS (m/z): 337.1 $[M + H]^+$.

4.1.1.23. 2-(4-(aminomethyl)piperidin-1-yl)-5-(2,3-dichlorophenyl)pyridin-3-amine (6w1)
White solid, yield 90%, mp 167-169 °C, ^{1}H NMR (400 MHz, DMSO-d_6): δ 7.65 (dd, J = 1.2 Hz, J = 8.0 Hz, 1H), 7.58 (d, J = 2.0 Hz, 1H), 7.42 (t, 1H), 7.35 (dd, J = 1.6 Hz, J = 7.6 Hz, 1H), 7.02 (d, J = 2.0 Hz, 1H), 4.90 (s, 2H), 3.45 (d, 2H), 2.61 (t, 2H), 2.49 (d, 2H), 1.80 (d, 2H), 1.61 (s, 2H), 1.27-1.41 (m, 3H); ^{13}C NMR (100 MHz, DMSO-d_6) δ 150.3, 140.0, 135.7, 134.7, 132.3, 130.0, 129.9, 129.5 (2C), 128.3, 120.7, 48.5 (2C), 47.8, 29.9 (3C); MS (m/z): 351.1 $[M + H]^+$.

4.1.1.24. 6-(4-(aminomethyl)piperidin-1-yl)-[3,3'-bipyridin]-5-amine (6x1)
Pale yellow solid, yield 90%, mp 170-172 °C, ^{1}H NMR (400 MHz, DMSO-d_6): δ 8.82 (d, J = 2.0 Hz, 1H), 8.55 (dd, J = 0.8 Hz, J = 4.8 Hz, 1H), 7.97 (d, J = 8.0 Hz, 1H), 7.93 (d, J = 2.0 Hz, 1H), 7.44-7.50 (m, 1H), 7.27 (d, J = 2.0 Hz, 1H), 4.94 (s, 2H), 3.46 (d, 2H), 2.63 (t, 2H), 2.52 (d, 2H), 2.26 (s, 2H), 1.80 (d, 2H), 1.26-1.44 (m, 3H); ^{13}C NMR (100 MHz, DMSO-d_6) δ 150.7, 148.1, 147.1, 136.5, 133.7, 133.6, 133.1, 127.9, 123.8, 118.1, 48.6 (2C), 47.9, 39.2, 29.8 (2C); MS (m/z): 284.2 $[M + H]^+$.

4.1.1.25. 5-(2,3-dichlorophenyl)-N^2-(piperidin-4-ylmethyl)pyridine-2,3-diamine (6y1)
White solid, yield 89%, mp 171-173 °C, ^{1}H NMR (400 MHz, DMSO-d_6): δ 7.57 (d, J = 7.6 Hz, 1H), 7.40 (s, 1H), 7.36 (t, 1H), 7.30 (d, J = 7.6 Hz, 1H), 6.77 (s, 1H), 5.84 (t, 1H), 4.91 (s, 2H), 3.18-3.33

(m, 3H), 2.97 (d, 2H), 2.46 (t, 2H), 1.70 (d, 3H), 1.01-1.15 (m, 2H); ^{13}C NMR (100 MHz, DMSO-d_6) δ 147.5, 140.9, 134.7, 132.2, 129.8, 129.2, 128.7, 128.1, 122.8, 117.7, 47.2, 45.6 (2C), 35.6, 30.8 (2C); MS (m/z): 351.1 $[M + H]^+$.

4.1.1.26. 2-(4-amino-4-methylpiperidin-1-yl)-5-(2,3-dichlorophenyl)pyridin-3-amine (6z1)
White solid, yield 87%, mp 164-166 °C, ^{1}H NMR (400 MHz, DMSO-d_6): δ 7.64 (d, J = 7.6 Hz, 1H), 7.59 (s, 1H), 7.42 (t, 1H), 7.37 (d, J = 7.6 Hz, 1H), 7.02 (s, 1H), 4.87 (s, 2H), 2.99-3.14 (m, 4H), 1.44-1.68 (m, 6H), 1.11 (s, 3H); ^{13}C NMR (100 MHz, DMSO-d_6) δ 150.2, 140.1, 135.5, 134.7, 132.3, 130.0, 129.9, 129.6, 129.4, 128.3, 120.7, 54.9, 46.8, 44.7 (2C), 39.6 (3C); MS (m/z): 351.1 $[M + H]^+$.

4.1.1.27. 2-(3-aminopiperidin-1-yl)-5-(2,3-dichlorophenyl)pyridin-3-amine (6a2)
White solid, yield 88%, mp 167-169 °C, ^{1}H NMR (400 MHz, DMSO-d_6): δ 7.65 (dd, J = 1.6 Hz, J = 7.6 Hz, 1H), 7.58 (d, J = 2.0 Hz, 1H), 7.42 (t, 1H), 7.36 (dd, J = 1.6 Hz, J = 7.6 Hz, 1H), 7.01 (d, J = 2.0 Hz, 1H), 4.98 (s, 2H), 3.28 (d, 1H), 3.17 (d, 1H), 2.89 (t, 1H), 2.71 (t, 1H), 2.51 (t, 1H), 2.33 (s, 2H), 1.80 (t, 2H), 1.56-1.70 (m, 1H), 1.14-1.30 (m, 1H); ^{13}C NMR (100 MHz, DMSO-d_6) δ 150.0, 140.0, 135.7, 134.6, 132.3, 130.0, 129.9, 129.6, 129.5, 128.3, 120.7, 57.2, 48.5, 47.5, 33.6, 23.3; MS (m/z): 337.1 $[M + H]^+$.

4.1.1.28. 6-(pyrrolidin-3-ylmethyl)-[3,3'-bipyridin]-5-amine (6b2)
White solid, yield 90%, mp 162-164 °C, ^{1}H NMR (400 MHz, DMSO-d_6): δ 7.58 (dd, J = 1.6 Hz, J = 8.0 Hz, 1H), 7.42 (d, J = 2.0 Hz, 1H), 7.37 (t, 1H), 7.31 (dd, J = 1.6 Hz, J = 8.0 Hz, 1H), 6.79 (d, J = 2.0 Hz, 1H), 5.97 (t, 1H), 4.95 (s, 2H), 3.93 (s, 1H), 3.26-3.42 (m, 2H), 2.87-2.98 (m, 2H), 2.75-2.84 (m, 1H), 2.59-2.67 (m, 1H), 2.39-2.48 (m, 1H), 1.80-1.91 (m, 1H), 1.39-1.51 (m, 1H); 13C NMR (100 MHz, DMSO-d6) δ 147.4, 140.8, 134.6, 132.2, 129.8 (2C), 129.3, 128.8, 128.1, 123.0, 117.7, 50.3, 45.8, 44.6, 38.4, 29.8; MS (m/z): 337.1 $[M + H]^+$.

4.1.1.29. N^2-(4-aminophenyl)-5-(2,3-dichlorophenyl)pyridine-2,3-diamine (6c2)
Pale yellow solid, yield 88%, mp 191-193 °C, ^{1}H NMR (400 MHz, DMSO-d_6): δ 7.59 (dd, J = 1.6 Hz, J = 7.6 Hz, 1H), 7.50 (s, 1H), 7.43 (t, 1H), 7.39 (t, 1H), 7.33 (d, J = 7.6 Hz, 1H), 7.30 (d, J = 8.4 Hz, 2H), 6.90 (s, 1H), 6.53 (d, J = 8.4 Hz, 2H), 5.12 (s, 2H), 4.73 (s, 2H); ^{13}C NMR (100 MHz, DMSO-d_6) δ 144.8, 143.2, 140.5, 134.3, 132.3, 130.8, 129.9 (2C), 129.8, 129.0, 128.2, 124.6, 121.7 (2C), 118.9, 114.0 (2C); MS (m/z): 345.1 $[M + H]^+$.

4.1.1.30. N^2-(4-aminophenyl)-5-(2-chlorophenyl)pyridine-2,3-diamine (6d2)
Pale yellow solid, yield 87%, mp 195-197 °C, ^{1}H NMR (400 MHz, DMSO-d_6): δ 7.52 (d, J = 7.6 Hz, 1H), 7.42-7.47 (m, 2H), 7.33-7.39 (m, 3H), 7.31 (d, J = 8.4 Hz, 2H), 6.93 (d, J = 1.6 Hz, 2H), 6.55 (d, J = 8.4 Hz, 2H), 5.10 (s, 2H), 4.72 (s, 2H); ^{13}C NMR (100 MHz, DMSO-d_6) δ 144.6, 143.1, 137.9, 134.3, 131.6, 131.3, 131.0, 129.9, 129.8, 128.5, 127.4, 124.7, 121.5 (2C), 119.3, 114.0 (2C); MS (m/z): 311.1 $[M + H]^+$.

4.1.1.31. N^2-(4-aminophenyl)-5-(3,4-dichlorophenyl)pyridine-2,3-diamine (6e2)
Pale yellow solid, yield 89%, mp 193-195 °C, ^{1}H NMR (400 MHz, DMSO-d_6): δ 7.78 (dd, J = 2.0 Hz, J = 8.0 Hz, 2H), 7.63 (dd, J = 2.0 Hz, J = 8.4 Hz, 1H), 7.57 (s, 1H), 7.54 (dd, J = 2.0 Hz, J =

8.4 Hz, 1H), 7.32 (d, *J* = 8.4 Hz, 2H), 7.13 (d, *J* = 2.0 Hz, 2H), 6.54 (d, *J* = 8.4 Hz, 2H), 5.13 (s, 2H), 4.75 (s, 2H); ^{13}C NMR (100 MHz, DMSO-d_6) δ 145.2, 143.2, 139.3, 132.7, 131.5, 130.9, 130.8, 130.8, 128.6, 126.9, 125.5, 123.3, 121.6 (2C), 116.0, 114.0 (2C); MS (m/z): 345.1 $[M + H]^+$.

4.1.1.31. N^2-(3-aminophenyl)-5-(2,3-dichlorophenyl)pyridine-2,3-diamine (6f2)
Pale yellow solid, yield 90%, mp 197-199 °C, ^{1}H NMR (400 MHz, DMSO-d_6): δ 7.61 (d, 2H), 7.52 (d, *J* = 2.0 Hz, 1H), 7.41 (t, 1H), 7.36 (d, *J* = 7.6 Hz, 1H), 7.00 (s, 1H), 6.96 (d, *J* = 2.0 Hz, 1H), 6.89 (t, 1H), 6.83 (d, *J* = 7.6 Hz, 1H), 6.16 (d, *J* = 7.6 Hz, 1H), 5.25 (s, 2H), 4.95 (s, 2H); ^{13}C NMR (100 MHz, DMSO-d_6) δ 148.7, 143.7, 142.3, 140.3, 134.1, 132.3, 130.8, 129.9 (2C), 129.9, 129.2, 128.6, 128.3, 125.8, 119.6, 107.2, 107.1, 104.5; MS (m/z): 345.1 $[M + H]^+$.

4.1.1.32. N^2-(3-aminophenyl)-5-(2,3-difluorophenyl)pyridine-2,3-diamine (6g2)
Pale yellow solid, yield 92%, mp 195-197 °C, ^{1}H NMR (400 MHz, DMSO-d_6): δ 7.58-7.65 (m, 2H), 7.52 (d, *J* = 2.0 Hz, 1H), 7.41 (t, 1H), 7.35 (d, *J* = 7.6 Hz, 1H), 7.00 (s, 1H), 6.96 (d, *J* = 2.0 Hz, 1H), 6.89 (t, 1H), 6.84 (d, *J* = 7.6 Hz, 1H), 6.16 (d, *J* = 8.0 Hz, 1H), 5.25 (s, 2H), 4.95 (s, 2H); ^{13}C NMR (100 MHz, DMSO-d_6) δ 150.4 (dd, *J* = 13.3 Hz, *J* = 243.6 Hz), 148.7, 147.1 (dd, *J* = 12.8 Hz, *J* = 244.8 Hz), 144.0, 142.2, 134.0 (d, *J* = 3.8 Hz), 132.7 (d, *J* = 101.9 Hz), 132.0 (d, *J* = 2.7 Hz), 131.4, 128.7, 124.9, 120.0, 118.8 (d, *J* = 2.7 Hz), 115.5 (d, *J* = 17.0 Hz), 107.3, 107.2, 104.6; MS (m/z): 313.1 $[M + H]^+$.

4.1.1.34. (2-(4-amino-4-methylpiperidin-1-yl)-5-(2,3-dichlorophenyl)pyridin-3-yl)methanol (11a)
White solid, yield 81%, mp 159-161 °C, ^{1}H NMR (400 MHz, DMSO-d_6): δ 8.19 (d, *J* = 2.0 Hz, 1H), 7.84 (d, *J* = 2.0 Hz, 1H), 7.67 (dd, *J* = 1.6 Hz, *J* = 7.6 Hz, 1H), 7.45 (t, 1H), 5.40 (dd, *J* = 1.6 Hz, *J* = 7.6 Hz, 1H), 5.40 (s, 1H), 4.50 (s, 2H), 3.07-3.26 (m, 4H), 1.45-1.62 (m, 4H), 1.10 (s, 3H); 13C NMR (100 MHz, DMSO-d6) δ 159.4, 145.2, 139.6, 137.1, 132.4, 130.0, 129.9, 129.7, 128.4, 127.3 (2C), 58.5, 46.8 (2C), 46.4 (3C), 30.3; MS (m/z): 366.1 $[M + H]^+$.

4.1.1.35. (2-(4-(aminomethyl)piperidin-1-yl)-5-(2,3-dichlorophenyl)pyridin-3-yl)methanol (11b)
White solid, yield 82%, mp 160-162 °C, ^{1}H NMR (400 MHz, DMSO-d_6): δ 8.21 (d, *J* = 2.0 Hz, 1H), 7.85 (s, 1H), 7.61-7.72 (m, 1H), 7.37-7.49 (m, 2H), 4.51 (s, 2H), 3.49 (d, 2H), 2.75 (t, 2H), 2.47 (d, 2H), 1.79 (d, 2H), 1.33-1.45 (m, 1H), 1.19-1.31 (m, 2H); ^{13}C NMR (100 MHz, DMSO-d_6) δ 159.6, 145.2, 139.5, 137.1, 132.4, 130.0, 129.9, 129.7, 128.4, 127.6, 127.6, 58.4, 50.2 (2C), 47.8, 30.0 (2C); MS (m/z): 366.1 $[M + H]^+$.

4.2. Biological evaluation

4.2.1 *In vitro* phosphatase activity assay

The purified SHP2 and SHP1 were used as the enzymes, and the peptide sequence EFpYAEVGRSPPDPAK (H-Glu-Phe-pTyr-Ala-Glu-Val-Gly-Arg-Ser-Pro-Pro-Asp-Pro-Ala-Lys) was used as the substrate[32]. The assay determined free phosphate generated by dephosphorylation of the substrate using the Malachite Green Phosphate Assay Kit. First, 0.4 mg/mLSHP2 or SHP1 protein, 0.06 mM substrate and assay buffer (25 mM Tris-HCl, 50 mM NaCl, 5 mM DTT, and 2.5 mM EDTA, pH 7.4) with the tested compounds at various concentrations were added in 96well plates at room temperature for 0.5 h. Subsequently, 25 μL NaOH (4 M) was added to the sample, and heated at 100 °C for 30 minutes and cooled to room temperature. Then, after the sample was

cooled to room temperature, 25 μL HCl (4 M) was added. Finally, 20 μL malachite green working reagent was added, and OD_{620} was measured after 0.5 h at room temperature. The IC_{50} value against SHP2 or SHP1 protein was gained. The result was analyzed by Graph-Pad Prism 7 software.

4.2.2. Fluorescence titrations

To verify whether the compound bound directly to the SHP2 protein, fluorescence quenching assay was used to examine change in the fluorescence of the SHP2 protein. The purified SHP2 his-fusion protein was diluted into reaction buffer with pH 7.4. The titration was carried out by increasing the concentration of the compounds while maintaining the SHP2 protein concentration at 0.4 mg/mL. The excitation wavelength was 295 nm, and fluorescence of 360 to 500 nm was monitored. All reported fluorescence intensities were relative values and were not corrected for wavelength variations in detector response.

4.2.3. Cell proliferation assay

Mouse B lymphocyte Ba/F_3 from the American Type Culture Collection (ATCC; Manassas, VA, USA) was incubated in RPMI 1640 (Gibco) medium supplemented with 10% fetal bovine serum (FBS; Origin South America sterile filtered), 1% penicillin-streptomycin, and 2 ng/ml murine IL-3 at 37°C in a humidified atmosphere of 5% CO_2. Cell growth was measured by MTT assay. Specifically, cells were seeded in 96-well plates at a density of 1.2×105 cells/mL and were untreated (control) or treated with test compounds solutions in 96-well plates. After incubation for 48 h, 20 μL/well MTT reagent was added and incubated for 4 h at 37°C. The reaction was stopped by adding 150 μL dimethyl sulfoxide. The absorbance density was obtained at wavelength 490 nm on a 96-well plate reader (NEST, Nest Biotechnology). IC_{50} value was calculated as the concentration of the drug required to obtain 50% of maximal inhibition in cell viability.

4.8. *In silico* ADMET prediction

The ADMET (absorption, distribution, metabolism, excretion, and toxicity) studies were performed using DS v3.5 software. Some important ADMET descriptors include human intestinal absorption (HIA)[33] (Prediction of drug absorption using multivariate statistics), plasma protein binding (PPB)[34] (Atomic solvation parameters applied to molecular dynamics of proteins in solution), aqueous solubility[35] (Prediction of aqueous solubility of a diverse set of compounds using quantitative structure-property relationships.), Cytochrome P450 2D6 binding (CYP2D6)[36] (Use of robust classification techniques for the prediction of human cytochrome P450 2D6 inhibition.), and hepatotoxicity[37] (In silico models for the prediction of dose-dependent human hepatotoxicity).

4.7. Molecular docking

Molecular docking study was performed by using the Discovery Studio 3.5 software. The X-ray crystal structure of SHP2 was derived from the RCSB protein database, identifier PDB ID: 5EHR. First, the preparation of proteins and the energy of the ligands was minimized by the CHARMm force field (). Subsequently, the receptor binding pocket was defined by the coordinate space of the extracted co-crystallized ligand[38] (Scaffold-based novel SHP2 allosteric inhibitors design using Receptor-Ligand pharmacophore model, virtual screening and molecular dynamics. Comput Biol Chem). The binding pocket of a protein was generally defined by a residue having at least one heavy atom, and the distance between this heavy atom and the heavy atom of the ligand was 5 Å[39]

(Design novel dual agonists for treating type-2 diabetes by targeting peroxisome proliferator-activated receptors with core hopping approach.). Finally, the docking module in the DS v3.5 program was performed to dock the ligands into the protein. The conformation with the highest docking score was used to analyze the interaction between the protein and the ligand.

CONFLICT OF INTEREST

The authors report no conflicts of interest in this work.

References

1. Hof, P., et al., *Crystal structure of the tyrosine phosphatase SHP-2.* Cell, 1998. **92**(4): p. 441-50.
2. LaRochelle, J.R., et al., *Structural reorganization of SHP2 by oncogenic mutations and implications for oncoprotein resistance to allosteric inhibition.* Nat Commun, 2018. **9**(1): p. 4508.
3. Barford, D. and B.G. Neel, *Revealing mechanisms for SH2 domain mediated regulation of the protein tyrosine phosphatase SHP-2.* Structure, 1998. **6**(3): p. 249-54.
4. Pluskey, S., et al., *Potent stimulation of SH-PTP2 phosphatase activity by simultaneous occupancy of both SH2 domains.* J Biol Chem, 1995. **270**(7): p. 2897-900.
5. Tartaglia, M., et al., *Mutations in PTPN11, encoding the protein tyrosine phosphatase SHP-2, cause Noonan syndrome (vol 29, pg 465, 2001).* Nature Genetics, 2002. **30**(1): p. 123-123.
6. Tartaglia, M., et al., *Somatic mutations in PTPN11 in juvenile myelomonocytic leukemia, myelodysplastic syndromes and acute myeloid leykemia (vol 34, pg 148,*

2003). Nature Genetics, 2003. **34**(4): p. 464-464.

7. Bentires-Alj, M., et al., *Activating mutations of the Noonan syndrome-associated SHP2/PTPN11 gene in human solid tumors and adult acute myelogenous leukemia.* Cancer Research, 2004. **64**(24): p. 8816-8820.

8. Chan, R.J. and G.S. Feng, *PTPN11 is the first identified proto-oncogene that encodes a tyrosine phosphatase.* Blood, 2007. **109**(3): p. 862-867.

9. Neel, B.G., H.H. Gu, and L. Pao, *The 'Shp'ing news: SH2 domain-containing tyrosine phosphatases in cell signaling.* Trends in Biochemical Sciences, 2003. **28**(6): p. 284-293.

10. Pan, J.H. and X. Liu, *[Assessment of landscape ecological security and optimization of landscape pattern based on spatial principal component analysis and resistance model in arid inland area: A case study of Ganzhou District, Zhangye City, Northwest China].* Ying Yong Sheng Tai Xue Bao, 2015. **26**(10): p. 3126-36.

11. Gavrieli, M., et al., *Characterization of phosphotyrosine binding motifs in the cytoplasmic domain of B and T lymphocyte attenuator required for association with protein tyrosine phosphatases SHP-1 and SHP-2.* Biochem Biophys Res Commun, 2003. **312**(4): p. 1236-43.

12. Scott, L.M., et al., *Targeting protein tyrosine phosphatases for anticancer drug discovery.* Curr Pharm Des, 2010. **16**(16): p. 1843-62.

13. Zeng, L.F., et al., *Therapeutic potential of targeting the oncogenic SHP2 phosphatase.* J Med Chem, 2014. **57**(15): p. 6594-609.

14. Zhang, X., et al., *Salicylic acid based small molecule inhibitor for the oncogenic Src*

homology-2 domain containing protein tyrosine phosphatase-2 (SHP2). J Med Chem, 2010. **53**(6): p. 2482-93.

15. Zeng, L.F., et al., *Therapeutic Potential of Targeting the Oncogenic SHP2 Phosphatase.* Journal of Medicinal Chemistry, 2014. **57**(15): p. 6594-6609.

16. Lawrence, H.R., et al., *Inhibitors of Src homology-2 domain containing protein tyrosine phosphatase-2 (Shp2) based on oxindole scaffolds.* Journal of Medicinal Chemistry, 2008. **51**(16): p. 4948-4956.

17. Noren-Muller, A., et al., *Discovery of protein phosphatase inhibitor classes by biology-oriented synthesis.* Proceedings of the National Academy of Sciences of the United States of America, 2006. **103**(28): p. 10606-10611.

18. Fortanet, J.G., et al., *Allosteric Inhibition of SHP2: Identification of a Potent, Selective, and Orally Efficacious Phosphatase Inhibitor.* Journal of Medicinal Chemistry, 2016. **59**(17): p. 7773-7782.

19. Chen, Y.N.P., et al., *Allosteric inhibition of SHP2 phosphatase inhibits cancers driven by receptor tyrosine kinases.* Nature, 2016. **535**(7610): p. 148-+.

20. Nichols, R.J., et al., *RAS nucleotide cycling underlies the SHP2 phosphatase dependence of mutant BRAF-, NF1-and RAS-driven cancers.* Nature Cell Biology, 2018. **20**(9): p. 1064-+.

21. Sarver, P., et al., *6-Amino-3-methylpyrimidinones as Potent, Selective, and Orally Efficacious SHP2 Inhibitors (vol 62, pg 1793, 2019).* Journal of Medicinal Chemistry, 2019. **62**(7): p. 3781-3781.

22. Bagdanoff, J.T., et al., *Optimization of Fused Bicyclic Allosteric SHP2 Inhibitors.*

Journal of Medicinal Chemistry, 2019. **62**(4): p. 1781-1792.

23. Krueger, B.A., et al., *Scaffold-Hopping Potential of Fragment-Based De Novo Design: The Chances and Limits of Variation.* Combinatorial Chemistry & High Throughput Screening, 2009. **12**(4): p. 383-396.

24. *The scaffold hopping potential of pharmacophores.* Drug Discov Today Technol, 2010. **7**(4): p. e203-70.

25. Hu, Y., D. Stumpfe, and J. Bajorath, *Recent Advances in Scaffold Hopping.* J Med Chem, 2017. **60**(4): p. 1238-1246.

26. Yang, J., et al., *Crystal structure of human protein-tyrosine phosphatase SHP-1.* J Biol Chem, 2003. **278**(8): p. 6516-20.

27. Norinder, U. and C.A. Bergstrom, *Prediction of ADMET Properties.* ChemMedChem, 2006. **1**(9): p. 920-37.

28. Gleeson, M.P., *Generation of a set of simple, interpretable ADMET rules of thumb.* J Med Chem, 2008. **51**(4): p. 817-34.

29. Egan, W.J. and G. Lauri, *Prediction of intestinal permeability.* Adv Drug Deliv Rev, 2002. **54**(3): p. 273-89.

30. Liu, J.L., et al., *Structural Determination of Three Different Series of Compounds as Hsp90 Inhibitors Using 3D-QSAR Modeling, Molecular Docking and Molecular Dynamics Methods.* International Journal of Molecular Sciences, 2011. **12**(2): p. 946-970.

31. Wang, M.Y., et al., *Synthesis, biological evaluation and 3D-QSAR studies of imidazolidine-2,4-dione derivatives as novel protein tyrosine phosphatase 1B*

inhibitors. European Journal of Medicinal Chemistry, 2015. **103**: p. 91-104.

32. Wu, X.Q., et al., *Small Molecule Inhibitor that Stabilizes the Autoinhibited Conformation of the Oncogenic Tyrosine Phosphatase SHP2.* Journal of Medicinal Chemistry, 2019. **62**(3): p. 1125-1137.

33. Egan, W.J., K.M. Merz, and J.J. Baldwin, *Prediction of drug absorption using multivariate statistics.* Journal of Medicinal Chemistry, 2000. **43**(21): p. 3867-3877.

34. Wesson, L. and D. Eisenberg, *Atomic solvation parameters applied to molecular dynamics of proteins in solution.* Protein Sci, 1992. **1**(2): p. 227-35.

35. Cheng, A.L. and K.M. Merz, *Prediction of aqueous solubility of a diverse set of compounds using quantitative structure-property relationships.* Journal of Medicinal Chemistry, 2003. **46**(17): p. 3572-3580.

36. Susnow, R.G. and S.L. Dixon, *Use of robust classification techniques for the prediction of human cytochrome P450 2D6 inhibition.* Journal of Chemical Information and Computer Sciences, 2003. **43**(4): p. 1308-1315.

37. Cheng, A. and S.L. Dixon, *In silico models for the prediction of dose-dependent human hepatotoxicity.* Journal of Computer-Aided Molecular Design, 2003. **17**(12): p. 811-823.

38. Jin, W.Y., et al., *Scaffold-based novel SHP2 allosteric inhibitors design using Receptor-Ligand pharmacophore model, virtual screening and molecular dynamics.* Computational Biology and Chemistry, 2018. **73**: p. 179-188.

39. Ma, Y., et al., *Design Novel Dual Agonists for Treating Type-2 Diabetes by Targeting Peroxisome Proliferator-Activated Receptors with Core Hopping Approach.* Plos One,

2012. **7**(6).

GA

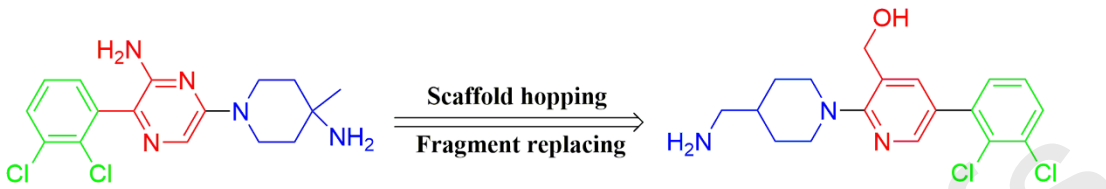

1 (SHP099)

11a
IC_{50} = 1.36 μM (SHP2)
IC_{50} > 100 μM (SHP1)
IC_{50} = 2.35 μM (antiproliferation)

Highlights

1. This manuscript was the first reported to design SHP2 inhibitors with 3-substituted pyridine as the core structure, and 35 new compounds were obtained.
2. In this manuscript, a series of biological evaluation were carried out on these 35 compounds, including *in vitro* enzyme activity, fluorescence titration and cell proliferation assays, and multiple inhibitors with good activity and development value were obtained.
3. In this manuscript, *in vitro* ADMET prediction investigated pharmacokinetic characteristics of these compound, and molecular docking study investigated the binding pocket of protein and ligand.

Conflict of Interest

The authors have declared no conflict of interest

Corresponding author: Run-Ling Wang Email: wangrunling@tmu.edu.cn